Leukemia (2020) 34:416–426
https://doi.org/10.1038/s41375-019-0582-x

ARTICLE

Acute myeloid leukemia

In vivo efficacy of mutant IDH1 inhibitor HMS-101 and structural resolution of distinct binding site

Anuhar Chaturvedi[1] · Ramya Goparaju[1] · Charu Gupta[1] · Julia Weder[2] · Thomas Klünemann[2] · Michelle Maria Araujo Cruz[1] · Arnold Kloos[1] · Kerstin Goerlich[1] · Renate Schottmann[1] · Basem Othman[1] · Eduard A. Struys[3] · Heike Bähre[4] · Denis Grote-Koska[5] · Korbinian Brand[5] · Arnold Ganser[1] · Matthias Preller[2] · Michael Heuser[1]

Received: 11 December 2018 / Revised: 1 July 2019 / Accepted: 23 July 2019 / Published online: 4 October 2019

Abstract

Mutations in *isocitrate dehydrogenase 1* (IDH1) are found in 6% of AML patients. Mutant IDH produces R-2-hydroxyglutarate (R-2HG), which induces histone- and DNA-hypermethylation through the inhibition of epigenetic regulators, thus linking metabolism to tumorigenesis. Here we report the biochemical characterization, in vivo antileukemic effects, structural binding, and molecular mechanism of the inhibitor HMS-101, which inhibits the enzymatic activity of mutant IDH1 (IDH1mut). Treatment of IDH1mut primary AML cells reduced 2-hydroxyglutarate levels (2HG) and induced myeloid differentiation in vitro. Co-crystallization of HMS-101 and mutant IDH1 revealed that HMS-101 binds to the active site of IDH1mut in close proximity to the regulatory segment of the enzyme in contrast to other IDH1 inhibitors. HMS-101 also suppressed 2HG production, induced cellular differentiation and prolonged survival in a syngeneic mutant IDH1 mouse model and a patient-derived human AML xenograft model in vivo. Cells treated with HMS-101 showed a marked upregulation of the differentiation-associated transcription factors CEBPA and PU.1, and a decrease in cell cycle regulator cyclin A2. In addition, the compound attenuated histone hypermethylation. Together, HMS-101 is a unique inhibitor that binds to the active site of IDH1mut directly and is active in IDH1mut preclinical models.

Introduction

Mutations in the active site arginine residue (R132) of *isocitrate dehydrogenase 1* (*IDH1*) have been found in about 6–10% of acute myeloid leukemia (AML) patients [1, 2], which confer a neomorphic function to the mutant enzyme and result in elevated levels of R-2-hydroxyglutarate (R-2HG) [3, 4]. IDH1 mutations lead to a block in cellular differentiation and promote tumorigenesis partly due to global DNA and histone hypermethylation by disruption of α-ketoglutarate dependent enzymes through R-2HG [5–7]. Thus, the inhibition of oncogenic

These authors contributed equally: Anuhar Chaturvedi, Ramya Goparaju

These authors contributed equally: Matthias Preller and Michael Heuser

Supplementary information The online version of this article (https://doi.org/10.1038/s41375-019-0582-x) contains supplementary material, which is available to authorized users.

✉ Matthias Preller
preller.matthias@mh-hannover.de

✉ Michael Heuser
heuser.michael@mh-hannover.de

[1] Department of Hematology, Hemostasis, Oncology and Stem Cell Transplantation, Hannover Medical School, Hannover, Germany

[2] Institute for Biophysical Chemistry, Hannover Medical School, Hannover and Centre for Structural Systems Biology, Hamburg, Germany

[3] Department of Clinical Chemistry, VU University Medical Center, Amsterdam, The Netherlands

[4] Research Core Unit Metabolomics, Institute of Pharmacology, Hannover Medical School, Hannover, Germany

[5] Institute of Clinical Chemistry, Hannover Medical School, Hannover, Germany

mutant IDH1 represents an opportunity for therapeutic intervention. The crystal structures reported from X-ray crystallographic studies are currently being used as protein models of choice to screen inhibitors which specifically target mutant IDH1, while sparing wild-type IDH1 [3]. Human cytosolic IDH1 consists of asymmetric subunits forming a dimer. The crystal structure of wild-type IDH1 consists of a large domain, a small domain and a clasp domain [8]. A deep cleft is formed by the large domain, the small domain and a second small domain from a different subunit, which together form the active site of the enzyme [8]. The hydrophilic active site has pockets for isocitrate, a metal ion, and NADP binding sites [8]. An amino acid change at arginine 132 in the active site to histidine or cysteine induces a conformational change leading to increased affinity to α-ketoglutarate, which is then catalyzed to R-2HG [9]. Thus, altered substrate-binding affinity confers a neomorphic function to the mutant IDH1 enzyme.

Several IDH1 inhibitors have been designed that can target the conformational change induced by a single-mutated amino acid, and some of the IDH1 inhibitors like AG-120, IDH-305, FT-2102, and BAY1436032 have entered clinical trials or even have been approved (AG120/ivosidenib) [10–16]. Crystal structures of several IDH1 inhibitors (chemically related BAY1436032, AG-881, IDH1-305, IDH1-125, and IDH1-146) in complex with mutant IDH1 have shown that they bind to allosteric pockets, inducing a conformational change and consequently inhibit the catalytic activity [12, 17–19]. Until now there is no approved or clinically active inhibitor, which binds to the active site of mutant IDH1. By computational screening of ~500,000 compounds, we have previously identified the IDH1 mutant-specific inhibitor HMS-101, which has shown efficacy towards IDH1 mutant cells in vitro [20].

In this study, we evaluated the antileukemic effect of HMS-101 in a syngeneic mutant IDH1 mouse model and patient-derived human AML xenograft models as well as performed biochemical and structural studies to evaluate the molecular mechanism of this compound. From this study, we conclude that HMS-101 binds to the active site of mutant IDH1, which is different from other IDH1 inhibitors, inhibits cellular proliferation and induces differentiation in IDH1 mutant leukemia cells.

Materials and methods

IDH activity assay

The enzymatic activity of pure IDH proteins was assessed by measuring the rate of consumption or the production of NADPH spectrophotometrically at 340 nm wavelength. A reaction mixture was prepared with 100 mM Tris, pH 7.4, 1% BSA, and 5 mM of $MnCl_2$ along with 250 µM NADPH as the co-factor for IDH1 and IDH2 mutants and 50 mM HEPES, pH 7.5, 150 mM NaCl, and 20 mM of MgCl2 along with 1 mM NADP for IDH1 and IDH2 wt enzyme catalysis. Reactions containing 500 nM of mutant IDH1 or mutant IDH2 proteins were initiated by adding 250 µM α-ketoglutarate as a substrate, whereas reactions containing 3 nM of wt IDH1 or wt IDH2 proteins were initiated upon addition of 4 mM isocitrate. All chemicals for the activity assays were purchased from Sigma-Aldrich (Munich, Germany). Efficacy of the drug was tested by incubating IDH1 proteins with increasing concentrations of HMS-101 or PBS (control) for 30 min prior to the experiment. Assays were performed with Multiskan FC (Life Technologies, CA, USA), and the specific activity was calculated from the slope value obtained from kinetic reactions.

Crystallization, data collection, and structure determination

Crystals of the IDH1mut-HMS-101 complex were obtained by co-crystallization of the purified IDH1mut protein with a concentration of 10 mg/ml in the presence of 2 mM HMS-101 by the sitting drop vapor diffusion method at 4 °C. The mixture was incubated for 30 min on ice and subsequently mixed with an equal volume of the reservoir solution (0.2 M di-ammonium citrate, 20% (w/v) PEG 3350) without the addition of NADP or α-ketoglutarate. The crystals were transferred to a cryoprotection solution containing reservoir solution mixed with 2 mM HMS-101 and additional 25% ethylene glycol, and subsequently flash-cooled in liquid nitrogen. Diffraction data were collected at beamline PROXIMA-1, Synchrotron SOLEIL, Gif-sur-Yvette, France. The dataset was processed using XDS [21], and the structure was solved by molecular replacement using Phaser [22] of Phenix [23] and the structure of IDH1 wt (pdb: 1T09) [8] as the search model. Structure refinement was carried out with Phenix and a random 5% of the data was excluded for cross-validation. Model building and validation was done using C*oot* [24]. The final coordinates were stored in the protein database [25] with the identification code 6Q6F.

In silico screening of IDH1mut inhibitors, compound preparation, retroviral vectors, and infection of primary bone marrow cells, cloning, expression, and purification of recombinant IDH1 mutant proteins, microscale thermophoresis, 2-hydroxyglutarate quantification, patient samples, clonogenic progenitor assay, antibodies for immunophenotyping and morphologic analysis, cell culture and treatment, cell viability and cell counts, pharmacokinetic and toxicity analysis of HMS-101, bone marrow transplantation, treatment and monitoring of mice,

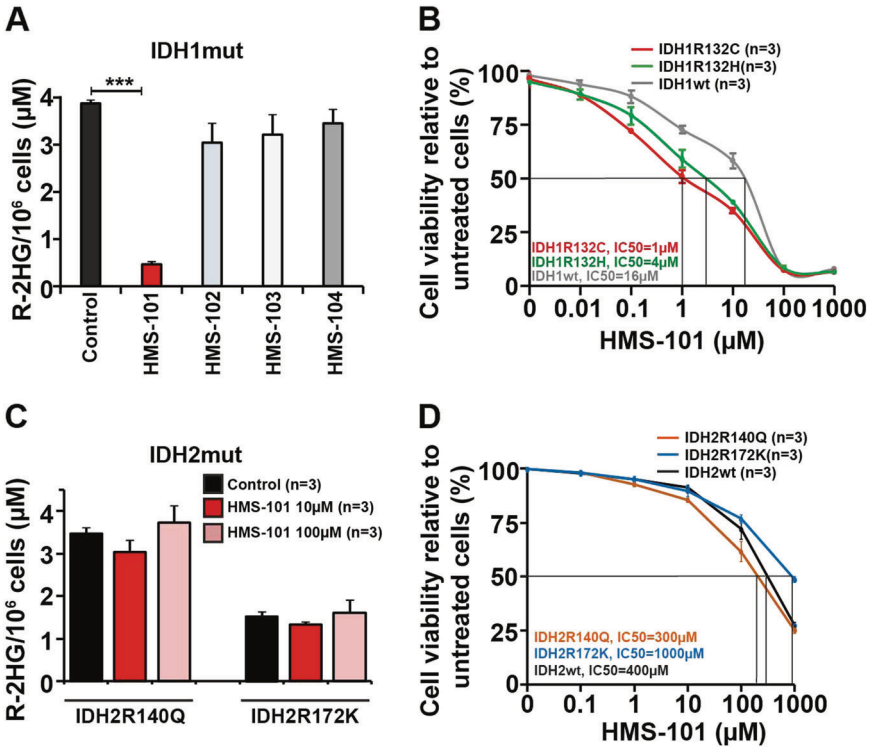

Fig. 1 Validation of candidate inhibitors of mutant IDH1. **a** Concentration of R-2HG per million cells in mouse HoxA9 + IDH1mut-transduced mouse bone marrow cells incubated with 10 μM of HMS-101, HMS-102, HMS-103, and 100 μM of HMS-104 or DMSO for 72 h (mean ± SEM, $n = 3$). **b** IC_{50} of HMS-101 in HoxA9 + IDH1 wt, HoxA9 + IDHmut R132C and HoxA9 + IDH1mut R132H cells treated for 72 h (mean ± SEM, $n = 3$). **c** Concentration of R-2HG per million cells in mouse HoxA9 + IDH2mut transduced mouse bone marrow cells incubated with 10 μM and 100 μM of HMS-101 or DMSO for 72 h (mean ± SEM, $n = 3$). **d** IC_{50} of HMS-101 in HoxA9 + IDH2 wt, HoxA9 + IDH2 R140Q, and HoxA9 + IDH2 R172K cells treated for 72 h (mean ± SEM, $n = 3$). ***$P < 0.001$

quantitative RT-PCR, immunoblotting and statistical methods are described in detail in Supplementary Materials.

Results

Validation of candidate inhibitors of mutant IDH1

A parallelized, high-throughput computational screening approach of ~0.5 million compounds from the Zinc database [26] against mutant IDH1, allowed us to identify four promising candidates for the specific inhibition of IDH1mut (Supplementary Table S1). These compounds showed high-binding energies against the high-resolution IDH1mut crystal structure (pdb: 3INM) [3] and a marked preference towards mutant IDH1 over wild type, when re-docked against an IDH1 wt crystal structure (pdb: 1T0L) [8]. We used a subset of the lead-like library of the Zinc database to ensure preferable pharmacokinetic properties of the compounds. Both, limiting the search area during computational docking to the isocitrate binding site, as well as covering both the isocitrate and NADP binding sites, suggested favorable binding of these ligands to the isocitrate binding pocket on IDH1mut with predicted binding energies in the range of −12 kcal/mol, giving computed ligand efficiencies (LE) of 0.5–0.8. In contrast, a second population was found for the larger search area with smaller parts of the ligands overlapping with the NADPH binding site, featuring slightly lower predicted overall binding energies. For both identified binding sites and all four compounds, the computed affinities towards IDH1mut were markedly higher than those obtained with IDH1 wt. The on-target efficacy of these candidate inhibitors was evaluated by their effect on R-2HG levels, which is specifically produced by mutant IDH1. Murine hematopoietic bone marrow cells were transformed with HoxA9 and the IDH1R132C mutant as described previously [20], and were treated with the four candidate IDH1 inhibitors for 72 h. The concentration of R-2HG was significantly reduced by HMS-101 and only slightly decreased by HMS-102, HMS-103, and HMS-104 (Fig. 1a and Supplementary Fig. S1A). We further evaluated their effect on cell viability in murine HoxA9 + IDH1mut cells expressing either the IDH1R132C or the IDH1R132H mutation. HMS-101 reduced the IC_{50} for both mutation types compared with IDH1 wild type-overexpressing cells, suggesting broad activity against different types of IDH1 mutations (Fig. 1b). However, HMS-101 did not inhibit R-2HG production in HoxA9 immortalized mouse bone marrow cells expressing IDH2 R140Q and R172K mutants (Fig. 1c and Supplementary Fig. S1B) and the cellular IC_{50} of HMS-101 was 300–1000-fold higher in IDH2 R140Q (300 μM), IDH2 R172K (1000 μM), and IDH2 wt (400 μM) cells compared with IDH1mut cells, indicating the specificity of HMS-101 towards mutant IDH1 (Fig. 1d). In order to determine the binding affinity of HMS-101 to IDH1mut, we used microscale thermophoresis measurements (Supplementary Fig. S1A). The binding affinity of HMS-101 toward IDH1mut in the absence of

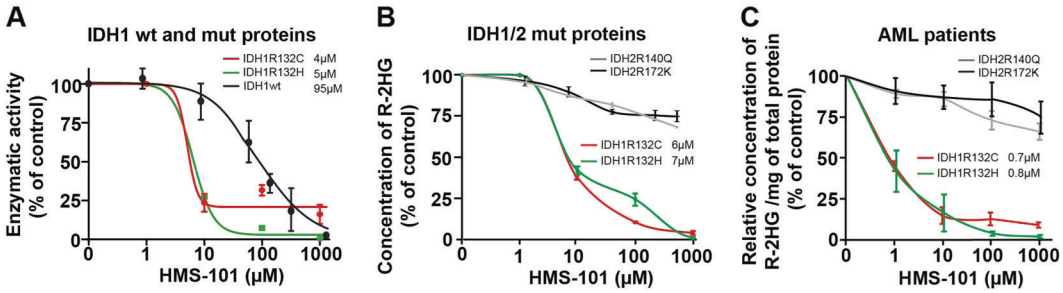

Fig. 2 HMS-101 inhibits the enzymatic activity of mutant IDH1. **a** Inhibition of IDH1mut R132C or IDH1mut R132H enzymatic activity measured by the rate of consumption of NADPH and IDH1 wt activity by the rate of production of NADPH in the presence of increasing concentrations of HMS-101 compared with the PBS treated control (mean ± SEM, $n = 3$). **b** Inhibition of R-2HG production by IDH1mut R132C, IDH1mut R132H, IDH2mut-R140Q, and IDH2mut-R172K proteins in the presence of increasing concentrations of HMS-101 compared with PBS-treated control (mean ± SEM, $n = 3$). **c** Concentration of R-2HG/mg protein in primary human AML cells harboring different IDH1 and IDH2 mutations 24 h after HMS-101 treatment, calculated as percentage of PBS control-treated cells. IC_{50} values for mutant IDH1 are provided in the graph (mean ± SEM, $n = 3$)

substrate and co-factor is in the low micromolar range (Kd: IDH1R132H 14.1 µM). In the presence of NADPH and αKG, the Kd of HMS-101 is shifted to higher values (Kd: IDH1R132H 445.9 µM and IDH1R132C 191.9 µM), indicating that HMS-101 competes with either NADPH or α-KG for binding to mutant IDH1. The other candidate inhibitors showed no differential cytotoxic effect in IDH1-mut compared with IDH1 wt cells (Supplementary fig. S2A–C). We, therefore, selected HMS-101 for further characterization.

HMS-101 inhibits the enzymatic activity of mutant IDH1

We purified His-tagged wild type and mutant IDH1 proteins (IDH1mut R132C and IDH1mut R132H) from the BL21DE3 bacterial strain (Supplementary Fig. S3). The preferential reactivity of the wild-type IDH1 protein with isocitrate and of the mutant IDH1 protein with αKG was confirmed in activity assays in vitro (Supplementary Fig. S4). While IDH1 wt and IDH2 wt enzymatic activities were only affected at higher compound concentrations (IC_{50}: IDH1 wt 95 µM, Fig. 2a, and IDH2 wt 110 µM, Supplementary Fig. S5), HMS-101 selectively inhibited the enzymatic activity of both IDH1 mutation types in a dose-dependent manner with an IC_{50} of 4 µM (IDH1mut R132C) and 5 µM (IDH1mut R132H), accounting for a 19- and 24-fold selectivity over IDH1 wt, respectively. The conversion from αKG to R-2HG by the IDH1mut pure protein in a cell free solution was also efficiently inhibited by HMS-101 (IC_{50}: IDH1mut R132C 6 µM, IDH1mut R132H 7 µM), however, the IC_{50} of HMS-101 was not reached until a concentration of 1 mM for the IDH2 mutant protein (Fig. 2b). We validated the specificity towards mutant IDH1 by treating primary AML cells from IDH1 and IDH2 mutated patients. R-2HG was reduced in a dose-dependent manner in IDH1 mutant but not in IDH2 mutant AML patients (IC_{50}: IDH1mut R132C 0.7 µM, IDH1mut R132H 0.8 µM, Fig. 2c). While R-2HG production was efficiently inhibited within 24 h, viability and cell counts of primary AML cells were hardly affected within this short time frame (Supplementary Fig. S6A, B). Thus, HMS-101 preferentially interferes with the enzymatic activity of mutant IDH1.

X-ray diffraction revealed the binding of HMS-101 in the active site of mutant IDH1

To verify the predicted binding of HMS-101 to the active site and to determine the detailed binding mode of the inhibitor, we co-crystallized IDH1mut R132H with HMS-101 in the absence of substrate or co-factor, and solved the structure by molecular replacement to a resolution of 3.3 Å (Fig. 3a). Statistics for diffraction data and structure refinement are shown in Supplementary Table S2. The overall fold of the IDH1mut-HMS-101 complex resembles the reported IDH1mut crystal structures, featuring a mutated homodimeric structure with an open/quasi-open active site conformation in the subunits and a width of the active site entrance of 19.7 and 17.0 Å (measured between residues 76 and 250 of the second subunit), respectively. Accordingly, the back clefts are closed with widths of 11.1 and 11.3 Å (measured between residues 199 and 342). The large domains of the subunits show the typical Rossmann fold, while the small domains fold in an α/β sandwich, and the clasp domains of the two subunits form together two four-stranded β-sheets. As has been seen before in crystal structures of IDH1mut in the open/quasi-open conformation (pdb: 3MAP and 3MAR) [9], the regulatory segment (seg-2, residues 271 to 286) in the active site is disordered and was not observable in the obtained HMS-101 complex crystal structure. This important structural segment, together with the hinge segment (seg-1, residues 134–141) undergoes substantial conformational rearrangements during the

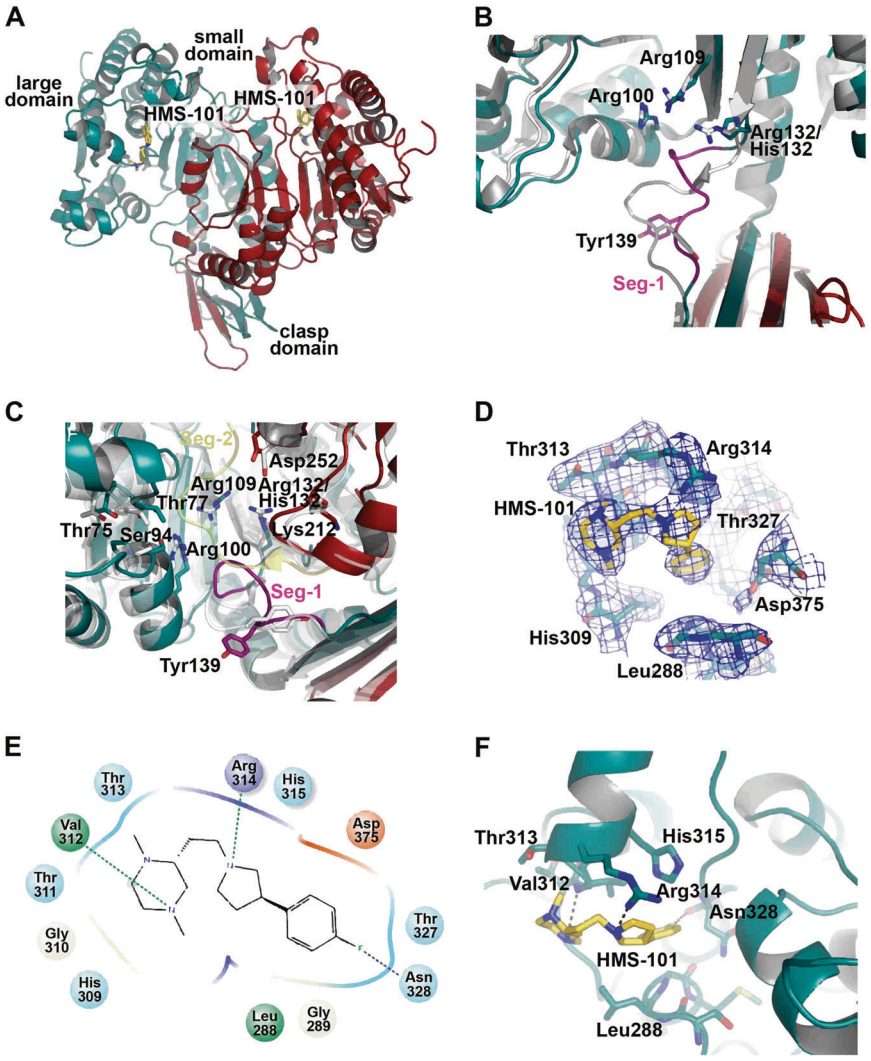

Fig. 3 Crystal structure of HMS-101 bound to the active site of mutant IDH1. **a** Overview of the co-crystallized structure of mutated IDH1 in complex with HMS-101 in a cartoon representation. The subunits of mutated IDH1 are depicted in cyan and red, and the inhibitor was found in both subunits. **b** Close-up view of segment-1 (seg-1, purple), featuring a slightly different conformation with rearrangements of the catalytically important residue Tyr139, as compared with the IDH1 wt crystal structure (pdb: 1T09, transparent gray structure). **c** Close-up view on the active site showing rearrangements of the active site residues that are involved in the enzymatic activity. Note the slightly more open active site due to the conformational changes of the large domain (cyan). The subdomains are colored cyan and red, seg-1, and seg-2 (of IDH1 wt crystal structure, pdb: 1T09) are shown in purple and yellow, respectively. For comparison, the IDH1 wt crystal structure is depicted as transparent gray structure. **d** The $2F_o$-F_c density map of HMS-101 and surrounding residues of the binding site. The map was contoured at 1.0 σ. **e** Interaction diagram, showing the HMS-101 binding site and contact residues. Green dashed lines indicate hydrogen bonds and purple dashed lines show halogen bonds. Color code: green: unpolar residues, red: negatively charged residues, purple: positively charged residues, cyan: polar residues, beige: glycine residues. **f** Close-up view of the HMS-101 binding site with contact residues shown as sticks. Dashed lines indicate favorable interactions with the protein

transition from the open conformation to the catalytically competent closed conformation [8]. Seg-1 could be resolved in our structure and adopts a slightly different conformation as compared with IDH1 wt in the open or closed state, with changes in the Tyr139 conformation (pdb: 1T09 and 1T0L, Fig. 3b) [8].

Compared with the known IDH1mut crystal structure in the presence of α-KG and NADPH (pdb: 3MAP), the large domains in the HMS-101-bound structure of both subunits are moved slightly outwards with root mean square deviations of 1.94 and 2.19 Å to adopt a slightly more open active site. Several rearrangements of active site residues were observed upon ligand binding, including residues Ser94, Arg100, Arg109, and Lys212 (Fig. 3c). The ligand HMS-101 binds to both subunits in a compact, bent conformation, and is nestled to a site that partially overlaps with the NADPH binding site in other known IDH1 crystal structures (Fig. 3a, d). Favorable interactions with protein

DOCKET ALARM

Explore Litigation Insights

Docket Alarm provides insights to develop a more informed litigation strategy and the peace of mind of knowing you're on top of things.

Real-Time Litigation Alerts

Keep your litigation team up-to-date with **real-time alerts** and advanced team management tools built for the enterprise, all while greatly reducing PACER spend.

Our comprehensive service means we can handle Federal, State, and Administrative courts across the country.

Advanced Docket Research

With over 230 million records, Docket Alarm's cloud-native docket research platform finds what other services can't. Coverage includes Federal, State, plus PTAB, TTAB, ITC and NLRB decisions, all in one place.

Identify arguments that have been successful in the past with full text, pinpoint searching. Link to case law cited within any court document via Fastcase.

Analytics At Your Fingertips

Learn what happened the last time a particular judge, opposing counsel or company faced cases similar to yours.

Advanced out-of-the-box PTAB and TTAB analytics are always at your fingertips.

API

Docket Alarm offers a powerful API (application programming interface) to developers that want to integrate case filings into their apps.

LAW FIRMS
Build custom dashboards for your attorneys and clients with live data direct from the court.

Automate many repetitive legal tasks like conflict checks, document management, and marketing.

FINANCIAL INSTITUTIONS
Litigation and bankruptcy checks for companies and debtors.

E-DISCOVERY AND LEGAL VENDORS
Sync your system to PACER to automate legal marketing.